Title: New mapping metrics to test functional response of food webs to coastal restoration

Authors: James A. Nelson[1*], J. Mason Harris[1], Justin S. Lesser[1], W. Ryan James[1], Glenn M. Suir[2], and Whitney P. Broussard III[3]

Author Affiliations:

[1]Department of Biology, University of Louisiana at Lafayette, Lafayette, LA

[2]Department of Geology, University of Louisiana at Lafayette, Lafayette, LA

[3]JESCO, Inc., Jennings, LA

***Corresponding Author:**

James Nelson
Department of Biology
University of Louisiana Lafayette
410 E. St. Mary Blvd.
Lafayette, LA 70504
Email: nelson@louisiana.edu

Key Words

landscape metrics, UAS, drone, saltmarsh, stable isotopes, mixing models, remote sensing

Abstract

The recovery of natural energy flow in food webs is an important indication that a restoration project has been a success, yet is typically considered a challenging component of post-restoration monitoring protocols. Advancements in remote sensing and SIA offer unique opportunities to build and test new metrics that more easily measure food web recovery following restoration. Here, we combine fine-scale remotely sensed data with SIA mixing model outputs to demonstrate a method for creating energetic landscape maps, or *E*-scapes, that assess the energetic quality of a multi-year marsh restoration effort for white shrimp (*Litopenaeus setiferus*). These maps explicitly link spatial features with the resources used by a consumer to allow managers to visualize and quantify how a restored landscape is producing energy for a target species. Our results support many known restoration paradigms concerning the relationship between habitat cover and use, highlighting its potential usefulness for monitoring purposes. With further testing and development, these products could also be used in the design of restoration projects and increase their potential for success.

1. Introduction

The primary goal of nearly all restoration efforts is to recover ecological function that has been lost due to some natural or anthropogenic disturbance (Higgs, 1997; Wortley et al., 2013). Ecological theory is central to restoration success and can help predict outcomes and track development over time (Zedler and Kercher, 2005). Restoration science is underpinned by several conceptual sub-disciplines of ecology; for example, community assembly theory suggests that initial restoration success and vegetation establishment can depend on the order of vegetation arrival and thus be guided by structured planting routines (Palmer et al., 1997). Succession is also a key component because a greater understanding of shifting biological communities following restoration actions informs timelines of site maturity (Prach et al., 2001).

Although diverse in design and implementation, most restoration efforts attempt to re-establish critical habitat(s) that support the desired suite of ecological or ecosystem functions (Suding, 2011; Wortley et al., 2013). Ecological restoration practitioners aim to create the environment necessary for recovery so the plants, animals, and microorganisms can conduct much of the recovery and create a more balanced system. Typical metrics of restoration success are often measured in some increase in the amount of desired habitat or an associated response in faunal presence in comparison to some reference location deemed to exhibit the desired functions (James et al., 2019; Neckles et al., 2002; Wortley et al., 2013). However, it has become clear that form does not always equal function when it comes to restoration success; areas deemed “restored” based on habitat metrics do not necessarily function as intended (Abelson et al., 2015). This is particularly true for the restoration of food web function; energy flowing from primary producers to upper trophic level consumers over multiple pathways does not always

72 track with the typical restoration metrics of presence/absence or abundance (James et al., 2019;
73 Moore and de Ruiter, 2012).
74 Food webs are inherently complex, understanding how energy flow responds to restoration is
75 difficult and costly (Ehrenfeld and Toth, 1997; Neckles et al., 2002). In the relatively few
76 examples of in-depth food web analysis following restoration, stable isotope analysis (SIA) is the
77 most commonly used tool to compare energy flow between restored and reference habitats
78 (Howe and Simenstad, 2007; James et al., 2019; Rezek et al., 2017b). The most common stable
79 isotopes used in restoration studies are carbon (^{13}C) and nitrogen (^{15}N). However, the use of
80 additional stable isotopes, such as sulfur (^{34}S) and hydrogen (D), could improve most
81 assessments (Layman et al., 2012). Stable isotopes are particularly attractive as a tool to monitor
82 restoration success because they can provide a time-integrated assessment of the flow of energy
83 in the food web. The isotope values can be used to identify and trace the production that
84 contributes to the food web and ultimately compare the primary energy sources used by the
85 restored and reference food webs. Most modern approaches use Bayesian mixing models to
86 assign food web contributions from sources in restored and reference habitats (Parnell et al.,
87 2013; Phillips et al., 2014). The primary benefit of these models is the incorporation of natural
88 variation in isotope value between sites which then provides better estimations of source
89 contributions (Parnell et al., 2013; Stock et al., 2018). Although few, studies that use SIA and
90 mixing models suggest that habitat complexes, the physical composition of the habitats, is one of
91 the most important components controlling food web recovery (James et al. 2019). This suggests
92 that linking the physical dynamics of habitats beyond the presence or absence of a specific
93 species or habitat class may be critical to understanding food web recovery.

Remotely-sensed landscape metrics are useful tools for quantifying large areas of habitat structure and understanding restoration development and trajectory. However, it is not always straightforward what the results of these metrics mean in terms of the ecology of a site (Kelly et al., 2011). Landscape ecology is based on the understanding of spatial arrangements within habitat mosaics and its influence on ecological phenomena (Wiens et al., 1993). Advancements in sensors and software have led to increased use of landscape metrics for assessing wetland configuration, fragmentation, and response to disturbance (Liu and Cameron, 2001; Stagg et al., 2019; Suir et al., 2013). Applying this type of study to restoration benefits developmental analysis by informing local and regional habitat structure, providing guidance for selection of reference sites, and improving knowledge of habitat configuration and variation based on scale (Taddeo et al., 2019). Drones or unmanned aircraft systems (UASs) offer a unique data stream that can help restoration practitioners understand the current state and future trajectory of a site. The technology has witnessed a rapid increase in ecological applications and a decrease in costs (Harris et al., 2019; Pajares, 2015). The resolution and variety of products that can be created from one drone survey have powerful implications for short and long-term site assessments. Fine-scale site maps can help address gaps in monitoring and provide a more ecological approach for essential principles like landscape context and position, comparisons to natural habitats, and responses to disturbance.

These advancements in remote sensing and SIA offer a unique opportunity to build and test new metrics of functional recovery following restoration. We combine fine-scale, remotely-sensed data from a multi-year marsh restoration effort with SIA mixing model outputs to create energetic landscape maps, or *E*-scapes (James et al. 2020, Harris et al. 2020). We use this method to predict which types of restoration design produces the most energetically-beneficial

117 landscape for white shrimp (*Litopenaeus setiferus*). *E*-scapes are species- or guild-specific
118 landscape maps that classify discrete areas on the landscape based on their energetic benefit to
119 the consumer(s) being considered. We hope this new type of analysis will be used to inform the
120 design of future restoration efforts to improve outcomes for restoring food web function.

121 **1. Materials and Methods**

122 *2.1 Site Description*

123 The Lake Sabine National Wildlife Refuge (SNWR) is the largest coastal marsh refuge on the
124 gulf coast. Located in southwestern Louisiana within the Calcasieu-Sabine Basin of the Chenier
125 Plain, the refuge encompasses 125,000 acres (about 500 km^2) of coastal wetlands. From 1956–
126 2006 this region lost over 900 km^2 of wetland, much of that within the SNWR (Barras et al.,
127 2008). In 2001, the Louisiana Coastal Protection and Restoration Authority designated nearly
128 6,000 acres in the SNWR for restoration due to the substantial marsh loss from canal-building
129 and altered hydrology, saltwater intrusion, and hurricanes. Four separate dredge-and-fill
130 restorations (known as Cycles 1–5) were completed between 2001 and 2015, restoring 1,120
131 acres of saltmarsh and shallow water habitat (Sharp 2011) (Figure 1 & 2). The project phases
132 were completed out of name order with Cycle 1 finished in 2002, Cycle 3 in 2007, Cycle 2 in
133 2010, and Cycle 5 in 2015. Cycle 4 is currently under construction and is not included in the
134 analysis. The fill material for each cycle was dredged from the Calcasieu Ship Channel by the
135 Army Corps of Engineers to maintain navigation access and then pumped into containment areas
136 to increase elevations and create new marsh. The dredge material slurry from the shipping
137 channel was to be pumped into each of the containment dikes to a maximum height of 70 to 140
138 cm and expected to settle to a height of 8 to 70 cm elevation after five years. While the general
139 parameters for each cycle were consistent, the construction techniques and final formations

140 varied, making them useful for comparisons of how different construction techniques alter the
141 functional outcomes for food web recovery.
142 We chose two reference natural marshes on the western boundary of the restoration areas for
143 comparisons. We chose these sites because they have been previously monitored by the Sabine
144 National Wildlife Refuge and they are the largest "intact" marsh systems near the area where the
145 restoration occurred. Reference North is a 50-hectare natural *Spartina patens*-dominated marsh
146 system with fringes of *Spartina alterniflora* along a tidal creek channel that splits the site evenly
147 north to south. Reference South is a 66-hectare natural marsh also dominated by *Spartina patens*
148 and dotted with small patches of water scattered evenly throughout the site.
149 Cycle 1 had an original containment of 86.6 hectares and was completed in February of 2002.
150 It is the oldest restoration site in this study (18 years). Sediment was pumped to an elevation
151 between 55 cm and 66 cm (Sharp 2011), it settled average elevation of 14 cm after 7 years (April
152 2009), and has been accreting at a rate of 0.4 cm/yr since 2010 (Basin, 2019). The most recent
153 average elevation reading was 18 cm (Basin, 2019). The site was built in the northeast corner of
154 the refuge, bounded by existing retention dikes on two sides, using approximately 765,000 cubic
155 meters of sediment pumped via a temporary pipeline from the Calcasieu Ship Channel. Cycle 1
156 was the only site that was planted, with thirty-six thousand smooth cordgrass (*Spartina*
157 *alterniflora*) plants established along the edges of the perimeter and the interior man-made
158 trenasses (small channels) manually dug during construction (Basin, 2019).
159 Cycle 3 was initially 93 hectares and completed in May of 2007 (Figure 2). It was pumped to
160 an elevation of 12 cm to 60.6 cm using 633,637 cubic meters of dredge sediment. Sediment was
161 incorrectly pumped into the containment area, causing the site to be higher in the south and
162 lower in the north with a wide range of surface elevations. The containment levees were

breached every 150 m on the northwest side to allow for the "spillover" delta formation component using sediment outflow; however, the technique did not work, and no additional marsh was gained. The site was surveyed in 2013 and had an elevation range of -62 cm to 25 cm, lower than the desired goal. By 2018 the site had accreted to an average elevation of 9 cm after 11 years. Aerial imagery, which was collected in 2009 and 2015, showed the area was 4.5% vegetated after 2 years and 97.8% vegetated cover after 8 years and dominated by *S. alterniflora* (Basin, 2019).

Cycle 2 had a containment area of 93 hectares, was completed in May 2010, and has less construction and historical monitoring data than other cycles because it was converted to a state of Louisiana-only project. Unlike other sites the desired "spillover" creation from breaching the containment levees was successful, creating an additional 40 hectares of marsh outside of the levee (Cycle 2 overflow). Limited field surveys reported the site to be an *S. alterniflora* monoculture and aerial imagery calculated it to be 77% land in 2015 (Suir et al. *in review*; Beck et al. 2019).

Cycle 5 is 94 hectares built with 565,000 cubic meters of dredge fill, but initial elevation measurements were not taken at the time of construction (Pontiff 2017). Three years after completion (2018) the elevation was reported to be between -11.8 cm and 26 cm (Miller 2019). Vegetation expanded rapidly post-construction and the site was 64% vegetated land within 9 months based on aerial imagery analysis from December 2015. *S. alterniflora* is the dominant species with nominal percentages of other plants throughout the site.

2.2 Habitat Mapping & Estimation

2.2.1 Unmanned Aircraft System (UAS) and flight parameters

All flights were conducted using a multi-rotor platform (Yuneec H520) designed for commercial purposes and chosen for this study because of high wind resistance, stability, and a long flight time (28 min). The flights occurred in the summer of 2019 from late June to mid-July between approximately 9:30 am–1:30 pm CDT. The flight area, time, altitude, and duration were configured using the internal autopilot flight planning software DataPilot. The internal Global Positioning System (GPS) module geotagged all images with an initial accuracy of 5 m horizontal and 8 m vertical. The hover accuracy of the aircraft was 1.5 m horizontal and 0.5 m vertical. The typical flight times ranged from 15 to 23 minutes.

We used a Yuneec E90 RGB camera equipped with a 23 mm lens with a diagonal field of view of 91° to capture all images used in the analysis. The photo resolution was 3:2 (5472 × 3648) and effective pixels were 20 MP. All photographs were stored as geotagged JPEG files on a micro SD directly inserted into the camera. The file size for each image was approximately 10–12 MB. Flight plans were developed using Yuneec DataPilot desktop mission planning software and uploaded to the ST16s remote controller before flight days. All flights were conducted at 68 meters altitude above ground level using consecutive transects to cover the survey areas with an image overlap of 80% (frontlap and sidelap). This altitude was chosen to maximize field of view while achieving <2.5 cm ground sample distance (GSD) or pixel resolution in the final maps for a precise analysis of vegetation classes and to minimize possible blurred portions (Broussard III et al., 2018).

We systematically chose ground control points (GCPs) around each site with at least one close to the center, in addition to randomly installed checkpoints throughout the study area. The *x*, *y*, and *z* coordinates of 69 points were taken with a Trimble R10 integrated GNSS system with an average error of 1.2 cm horizontal and 2.1 cm vertical. In total, 46 targets were used as control

points for georeferencing the imagery, and 23 targets were reserved as horizontal and vertical checkpoints to help assess the accuracy of the data. In general, 6 GCPs and 3 checkpoints were used at each site based on software manufacturer recommendations (Pix4D Mapper) and previous studies (Manfreda et al., 2019; Oniga et al., 2018).

2.2.2 Field Surveys

To verify the remotely sensed data and compare the sites using traditional monitoring methods we used 3 replicate 2 × 2 m quadrats sampled along a transect from the edge of each site moving toward the center at 1, 100, and 200 m for a total of nine quadrats per site. We recorded the species composition, plant height, and percent cover of the vegetated and unvegetated surfaces. This methodology was chosen based on the Braun-Blanquet cover scale (Kent, 2011) used by the USGS Coastwide Reference Monitoring System (Steyer, 2010) and CPRA protocols that have been used to monitor these sites in the past (Folse et al., 2012; Miller, 2014).

2.2.3 Imagery Processing and Analysis

The flights produced several thousand images per site that were post-processed using structure from motion (SfM) photogrammetry software Pix4D Mapper to create orthomosaics and digital surface models (DSMs). Orthomosaics are detailed, scaled, georeferenced photo representations of the area constructed from multiple images and DSMs are representations of the surface elevation and the tallest objects like vegetation or structures (Figures 2 and 3). We uploaded the GCP measurements with x, y, and z coordinates and horizontal and vertical precision error values, and the targets were manually clicked to verify the individual pixel center of targets using the ray cloud editor. Manual tie points (MTPs) were also added in the ray cloud to improve reconstruction accuracy and clarity in the final orthomosaic. We conducted all the

image processing on a Dell Precision Tower 5810 desktop with 32 GB of RAM, an Intel Xeon CPU E5-1603 v3 @ 2.80GHz, and an NVIDIA Quadro M2000 GPU. Processing times ranged from 36–72 hours per site. A total of 20,515 raw images were processed to create 1,694 acres of mapped area with an average GSD (pixel size) of ~2.2 cm (excluding Cycle 4, which is still under construction).

2.2.4 Classification

Two products were created by combining the orthomosaics and DSMs: (1) land/water maps and (2) habitat classifications. Land and water classes were delineated based on rules developed by Cowardin et al. (1979) where land was considered all vegetation including marsh, scrub/shrub, emergent vegetation, and exposed bare ground on the containment dikes (which is higher elevation and does not flood). Water was considered open water, non-vegetated mudflats, floating aquatics (which were minimal), and submerged aquatic vegetation. To compare the construction techniques between restoration cycles, the habitats in each site were characterized as water, edge, or marsh. Each of the restoration sites contained small areas of construction artifacts that created anomalous landscape features often occupied by nonstandard marsh plants; we classified these areas as "other" and excluded them from the analysis.

An object-based image analysis (Laliberte and Rango, 2011, 2009) was used to conduct vegetation mapping with the software eCognition Developer (v. 9.5, Trimble Germany GmbH, Munich, Germany). The orthomosaics and digital surface models provided four layers to use in image analysis (red, green, blue, and DSM). Each site was analyzed independently and separate "rulesets" were developed, using similar approaches and parameters, to assign classes to cover types. The rulesets are a step by step process of segmentation (grouping pixels into meaningful shapes, e.g., water bodies or trees) to create objects and classification of those objects based on

attributes, or “features” in eCognition, unique to the target class. Cycles 3 and 5 and Reference South were completely automated using ruleset development which included a supervised classification as the last step and no manual editing needed. Cycle 1, Cycle 2, and Reference North were classified using one round of segmentation, basic rules to separate bare ground, marsh vegetation, water, and additional manual editing. Initial features used to define classes were mean brightness, mean red band, mean DSM, roundness, area, and position values for individual objects. Misclassified areas were identified and reclassified through additional thresholding of other parameters or manually edited into the appropriate cover type. We exported the vector layers with the area (m^2) and border length (m) included in the attribute table and transferred to ArcGIS (ArcMap 10.4.1) for further spatial analysis and final cartography. The attribute tables were exported as spreadsheets and aggregated and analyzed using the R package ‘tidyverse’. We conducted accuracy assessments using stratified random sampling methods with 525 test points per site (QGIS). The number of points per class was weighted based on the percent cover within the site however we required each class had a minimum of 25 points.

2.3 Structural Analysis

Remotely sensed class areas, percentage of landscape, number of patches, patch density, edge density, and aggregation index (AI) were calculated based on usage in previous studies (Broussard et al. 2018). Patch AI has become a widely used metric for evaluating landscape structure and is a percentage calculated from the ratio of the observed number of patch type adjacencies (McGarigal 2015; Couvillion et al. 2016). Edge habitat in this study was considered the marsh-to-water border. Since the sites were cropped to the marsh edge and no water was classified outside the boundaries, the border length of the water class was used as a proxy for interior edge habitat. Exterior edge habitat was simply the total length of the land class minus the

amount of interior. Portions, where continuous habitat was cut off due to flight coverage, were measured and subtracted from total edge calculations. Removing the water also ensures the sites are only classified using the water within the borders of the restoration and it is not confounded by water or edge ratio around the perimeter. All landscape configuration metrics were calculated using R package Landscape Metrics that was developed from the program FRAGSTATS. The shapefiles created in eCognition were turned into raster format using the R package 'fasterize' so that spatial metrics could be analyzed. Vector files were rasterized to the original resolution of the mosaics used to conduct classifications. Correlations of these metrics were analyzed with ground survey data to determine any relevant trends for understanding marsh creation development in addition to restored vs reference comparisons.

2.4 Stable Isotope Analysis

For our analysis, we used white shrimp (*Litopenaeus setiferus*) as a model species to demonstrate how we can measure the ability of restoration landscapes to produce energy for the food web. The stable isotope analysis and mixing model methods and results used for this analysis are published in Nelson et al. (2019). Nekton were collected in August 2016 using a 1 m^2 drop sampler (Zimmerman et al.1984, Nelson et al. 2019), dried for 48 hours at 60 °C, ground into a fine powder, and shipped to the Washington State University Stable Isotope Core Facility for C, N, and S content and stable isotope analysis. The mixing model used particulate organic matter to represent water column production, *Spartina alterniflora* leaves to represent marsh production, *Avicennia germinans* leaves to represent mangrove production, and benthic epiphytes to represent benthic algal production.

The relative contribution of each organic matter source to white shrimp was derived using a Bayesian mixing model. All stable isotope data were analyzed in R (v 4.0.0, R Development

300 Core Team) using the package 'mixSIAR' (v 3.1.7, Stock et al. 2018). The mixing model
301 showed that mangrove production accounts for less than 1% of production and was excluded
302 from this analysis because there are no mangrove habitats on these sites (Nelson et al. 2019).

303 *2.5 Energetic Landscape Maps*

304 We applied the mixing model results for white shrimp to each of the drone-based habitat
305 assessments. A detailed description of the energetic landscape construction with an in-depth
306 description and test of the underlying assumptions can be found in James et al. (2020). The
307 habitat cover estimates developed from the UAS imagery were combined with consumer
308 resource use from the mixing models to calculate an index of energetic importance (IEI) for each
309 basal resource and habitat type combination. Each IEI was calculated with the following
310 formula:

311 $$IEI_i = \frac{f_{so}}{f_{habitat}}$$

312 where f_{so} is the fraction of the contribution of source *i* to the total source use based on the
313 results of the mixing model and $f_{habitat}$ is the fraction of habitat *i* that produces source *i* to the
314 overall area within the movement range of the consumer. An example of resource/habitat
315 combination is the amount of *S. alterniflora* derived production and the coverage area of *S.*
316 *alterniflora* marsh habitat. The IEI provides a value for the amount of a resource that a consumer
317 uses relative to the amount of that habitat in the foraging area where that consumer was captured.
318 An IEI of one indicates the consumer is using a resource (f_{so}) in the same proportion it
319 occurs in the area where it forages. If the IEI is greater than one, that resource is being used more
320 than expected based on its distribution in the foraging area. IEI values were combined with
321 habitat cover areas to calculate the habitat resource index (HRI). HRI was calculated with the
322 following formula:

$$HRI = \sum_{i=1}^{n} \widetilde{IEI}_i * f_{habitat}$$

where $\widetilde{IEI}_i$ is the median of the IEI for the source/habitat combination *i* and $f_{habitat}$ is the fraction of habitat *i* to the overall area within the movement range of the consumer. HRI is an index that represents a relative measurement of the quality of the habitats for producing the collection resources used by the consumer based on stable isotope analysis. An HRI value of one means that the area is producing resources proportional to the mean contribution of each production source used by the consumer as determined with the mixing model.

Each restoration cycle was divided into 400 m × 400 m (16 ha) habitat blocks to calculate the HRI for white shrimp. This value was chosen based on typical movement ranges of white shrimp in the field (Nelson et al., 2019; Rozas and Minello, 1997; Webb and Kneib, 2004). Sensitivity analysis in James et al. (2020) showed a significant relationship between shrimp biomass and HRI from 50 m^2 to 1000 m^2 scales.

3.0 Results

3.1 Habitat Assessment Results

The proportion of land at each site varied from 73.2% to 95.5% with the youngest cycle (Cycle 5) having the lowest proportion of land and the oldest site (Cycle 1) the highest. Both reference sites were approximately 91% land (Table1). All of the sites had aggregation indexes higher than 98% indicating the patches identified by the software were highly clumped and easily discernable from adjacent classes (Table 1).

The drone-based habitat assessments indicate the restoration sites were 74–90% covered by marsh vegetation. The youngest site, Cycle 5 (4 years old), was 90 ha and had the lowest proportion of marsh cover (74%) with the remaining 26% covered by water. The oldest site,

345 Cycle 1 (18 years old), was 108 ha and had the highest amount of marsh cover (90%). It also had
346 the highest percentage of shrubs and *P. australis* ("other" class) at 6%. The other two restoration
347 sites, Cycles 2 and 3, were 84–85% marsh-covered. Cycle 2 (9 years old) was 138 ha and Cycle
348 3 (12 years old) was 93 ha (Table 2). Cycle 2 was the largest site and contained the most marsh
349 (117 ha) because of the successful sediment overflow technique. The reference sites were both
350 88% marsh, 8–9% water, and 3–4% "other." Reference North was 50 ha and Reference South
351 was 66 ha.
352
353 *3.2 Mixing Model Results*
354 Benthic algae supported 49.2% (± 3.7 %) of white shrimp biomass. Water column production
355 (38.1% ± 6.8 %) was the second most important component supporting shrimp biomass,
356 followed by *Spartina* detritus (12.5% ± 3.6%). Mangrove production was not included in this
357 analysis as the mixing model determined mangroves contributed less than 1% to shrimp biomass
358 and there is no mangrove habitat on the restoration sites (Nelson et al. 2019).
359 *3.3 Energetic Landscape Results*
360 IEI values for edge and water were around 5 at most sites and were much higher than marsh,
361 which had IEI values <1 at all sites (Figure 4). Each site contained areas of higher and lower
362 energetic quality depending on the physical parameters in that cell of the *E*-scape (Figure 3). The
363 median HRI value for the *E*-scape sampling unit across all sites was 1.11 with an interquartile
364 range of 0.38–1.99. HRI values displayed a negative relationship with the proportion of total
365 land and the proportion of marsh habitat within the *E*-scape sampling unit (Figure 5,
366 supplemental figures). There was a positive relationship between HRI and the proportion of
367 landscape edge habitat with the *E*-scape sampling unit (Figure 5).

4.0 Discussion

For habitat restorations, the recovery of natural energy flow patterns is an important ecosystem function that may indicate a restoration project has been a success. However, post-restoration monitoring efforts have focused little on understanding energy flow and trophic dynamics (Ehrenfeld and Toth, 1997; Neckles et al., 2002), as food webs are complex and their structure is hard to monitor (Vander Zanden et al., 2006). By combining stable isotope information on energy flow with remotely-sensed landscape metrics, our method provides a clearer and deeper inferential method of assessing whether a project has restored food web function. Further, we feel our results demonstrate the utility of our method in evaluating how different construction methods would impact food web recovery. Our results indicate the importance of geomorphology or habitat form and support many known restoration paradigms concerning the relationship between habitat cover and species use, highlighting its usefulness for monitoring purposes.

Edge habitat has been well-established as an important driver of consumer biomass and abundance in saltmarshes (Minello et al., 1994; Webb and Kneib, 2002). Our *E*-scapes demonstrate the importance of this edge habitat to energy flow through white shrimp in these restored habitats (Figure 3). Edge habitat had high index of energetic importance (IEI) values at all sites because of the outsized reliance on the resource it produces (benthic algae) (Litvin et al., 2018) relative to the amount of edge area that exists at each site. While benthic algal production likely occurs across much of the marsh surface, the shallow edge habitat where light penetrates to the bottom has the highest concentration of benthic algal production and has been shown to be

390 an important area for marsh consumers (Kneib 2003). Therefore, areas with more edge are
391 energy-rich for shrimp, leading to a positive relationship between edge area and HRI values.
392 Cycles 1 and 2 were most similar to the energetic values of the reference habitats (Figure 3).
393 Both of these sites have greater water-to-edge ratio due to the construction techniques used to
394 create them. In Cycle 1 the areas with the trenasses have much higher HRI values than areas of
395 the site that were not trenched (Figure 3A). Cycle 2 is the site where the "spillover" technique
396 was successful and the spillover area has some of the highest HRI values of any of the study sites
397 due to the highly reticulated habitat structure and high edge ratio (Figure 2B). Conversely, marsh
398 habitat has consistently low energetic importance at all sites. Cordgrass productivity is typically
399 incorporated into the food web through the detritus pathway (Nelson et al., 2019), and white
400 shrimp do not rely on this pathway heavily (Nelson et al. 2019). Thus, restoration through the
401 creation of cordgrass habitat (and land overall) does not directly promote the provision of energy
402 for the food web as a function of total areas (Figure 4 and 5). This observation demonstrates a
403 critical consideration for restoring food web function, the structure created by the macrophyte is
404 critical to creating the areas that generate the most energetically-valuable areas of the habitat.
405 Frequently the success of restoration efforts, particularly in Louisiana, are measured in new land
406 created and amount of habitat restored. However, the geomorphology and structure of the habitat
407 is a key feature to consider when designing a restoration to promote recovery of food web
408 function.
409 Managers can use this tool during monitoring to assess the energetic health and progress of
410 establishing food webs in their restored site without major changes to their established data
411 collection programs. Post-restoration food web analysis is already typically done via stable
412 isotope analysis (James et al., 2019; Rezek et al., 2017b, 2017a). Remote sensing (via

drone/UAVs or satellite imagery) is a tool widely employed to monitor the establishment, progression, and recovery of areas to reference levels of habitat cover (Klemas, 2013). E-scapes combine these sets of data to produce a visual product that imparts new information about the progress of the pattern of energy flow at a restoration site. E-scapes can be tailored for target species to assess the success of a restored landscape in producing the collection of energy channels that support consumers that meet specific restoration goals (Harris et al. 2020). E-scapes can also be used to visualize variability in energy production across different parts of the restored landscape, leading to better design and construction of restoration habitats planned to restore natural energy flow patterns and trophic dynamics.

When combined with ecological models or indices, remotely-sensed data have much promise as a scientific monitoring tool. For this study, the use of UAS imagery in conjunction with the IEI, for the quantification and monitoring of wetland ecosystem goods and services, demonstrates the increased value for evaluating the performance of wetland restoration on food web function and energy flow. With near-term technological improvements (e.g., fusing of UAS-collected hyperspectral imagery and LiDAR data), UAS applications will become increasingly critical for environmental monitoring and research.

With advances in the spatial and spectral resolution of remotely sensed data from UAS, aircraft, and satellite technology, high-resolution maps and fine-scaled indices are possible that resolve the smallest ponds and pockets of the marsh landscape. Access to these products is now available through off-the-shelf drone technology and automated software workflows. Traditional tools and methods for quantifying energy flow through these newly resolved models will need to be adapted and scaled up.

5.0 Limitations and Future Considerations

436 As with any new methodology, there are several assumptions and methods that can be
437 improved in later iterations to better capture how energy is flowing in the system. For example,
438 in our calculation of HRI and IEI values, the fraction of habitat ($f_{habitat}$) is based on the area of
439 habitat cover. This means that all habitat of that type will produce energy equally and in two
440 dimensions. For aquatic habitats this can be problematic given the patchy nature of certain types
441 of production, or how depth and light penetration modulate productivity when considering water
442 column production. In addition, our habitat classifications are simplistic with a patch receiving a
443 single classification. In the real-world multiple production sources could occur on the same patch
444 (e.g. benthic algal production between cordgrass stems). Scale is also a critical assumption in our
445 approach. In this example we use shrimp home range information to determine the scale at which
446 the consumer uses resources to generate our metrics. For organisms that move at much larger
447 scales how the habitat cover types are classified and aggregated becomes more complex as
448 increasing numbers of sources and habitat types are incorporated. Our methods can easily be
449 adapted to consider these factors by adjusting habitat productivity by depth or with data, such as
450 chlorophyll concentration, over time. Movement and diet information could be used to identify
451 the proper scales and identify habitats used for foraging. Although these types of data do not
452 currently exist for our study area, technological advances in remote sensing, videography, and
453 animal tracking make attaining this information more feasible than ever.
454 Stable isotope analysis has been shown to be a powerful tool to understand how food webs
455 respond to change. With the recent technological advancements in fine-scale remote sensing
456 technology, we feel the time is right to begin to combine these two powerful tools to illuminate
457 spatial patterns in energy flow that had been previously unattainable. While our initial efforts

may be limited is some ways, they provide a framework to build toward a potentially powerful tool for assessing and planning coastal zone restoration projects.

Acknowledgments

We acknowledge Laura McDonald, Holly Mayeux for assistants processing samples in the laboratory. Juan Salas, Lawrence Rozas, Shawn Hillen for the field collections. We thank Benjamin Harlow for stable isotope analysis.

Funding sources

This work was supported by the National Oceanic and Atmospheric Administration, National Marine Fisheries Service, University of Louisiana Lafayette. Louisiana Sea Grant, and The National Academies of Science, Engineering, and Medicine Gulf Research Program. The funding sources had no role in the preparation of the article, study design, analysis, or the decision to submit the article for publication.

Declarations of interest

None.

Conflict of interest

There are no conflicts of interest concerning our article.

Literature Cited

Abelson, A., Halpern, B.S., Reed, D.C., Orth, R.J., Kendrick, G.A., Beck, M.W., Belmaker, J., Krause, G., Edgar, G.J., Airoldi, L., Brokovich, E., France, R., Shashar, N., de Blaeij, A., Stambler, N., Salameh, P., Shechter, M., Nelson, P.A., 2015. Upgrading Marine Ecosystem Restoration Using Ecological-Social Concepts. BioScience 66, 156–163. https://doi.org/10.1093/biosci/biv171

Barras, J.A., Bernier, J.C., Morton, R.A., 2008. Land area change in coastal Louisiana, a multidecadal perspective (from 1956 to 2006). US Department of the Interior, US Geological Survey Louisiana, US.

Basin, C.-S., 2019. 2019 Basin Summary Report.

Beck HJ et al. (2019) Sabine Refuge Marsh Creation (CS-28): 2015 land-water classification. U.S. Geological Survey

Broussard III, W., Suir, G.M., Visser, J.M., 2018. Unmanned Aircraft Systems (UAS) and Satellite Imagery Collections in a Coastal Intermediate Marsh to Determine the Land-Water Interface, Vegetation Types, and Normalized Difference Vegetation Index (NDVI) Values. ERDC VICKSBURG United States.

Ehrenfeld, J.G., Toth, L.A., 1997. Restoration ecology and the ecosystem perspective. Restoration ecology 5, 307–317.

Folse, T.M., West, J.L., Hymel, M.K., Troutman, J.P., Sharp, L.A., Weifenbach, D., McGinnis, T., Rodrigue, L.B., 2012. A standard operating procedures manual for the CoastWide Reference Monitoring System-Wetlands.

497 Harris, J.M., Nelson, J.A., Rieucau, G., Broussard III, W.P., 2019. Use of Drones in Fishery
498 Science. Transactions of the American Fisheries Society 148, 687–697.
499 https://doi.org/10.1002/tafs.10168
500 Harris, J. M., W. R. James, J. S. Lesser, J. C. Doerr, and J. A. Nelson. (2020*)*. Foundation
501 species shift alters the energetic landscape of marsh nekton. *Estuaries and Coasts*.
502 Higgs, E.S., 1997. What is Good Ecological Restoration? ¿ Que es una Buena Restauración
503 Ecológica? Conservation biology 11, 338–348.
504 Howe, E.R., Simenstad, C.A., 2007. Restoration trajectories and food web linkages in San
505 Francisco Bay's estuarine marshes: a manipulative translocation experiment. Marine
506 Ecology Progress Series 351, 65–76.
507 James, W.R., Lesser, J.S., Litvin, S.Y., Nelson, J.A., 2019. Assessment of food web recovery
508 following restoration using resource niche metrics. Science of The Total Environment
509 134801.
510 James WR, Santos RO, Rehage JS, Doerr JC, & JA Nelson 2020. *E*-scape: consumer specific
511 energetic landscapes derived from stable isotope analysis and remote sensing. *bioRxiv*
512 Kelly, M., Tuxen, K.A., Stralberg, D., 2011. Mapping changes to vegetation pattern in a
513 restoring wetland: Finding pattern metrics that are consistent across spatial scale and
514 time. Ecological Indicators 11, 263–273.
515 Kent, M., 2011. Vegetation description and data analysis: a practical approach. John Wiley &
516 Sons.
517 Klemas, V., 2013. Airborne remote sensing of coastal features and processes: An overview.
518 Journal of Coastal Research 29, 239–255.

519 Kneib, R. T. 2003. Bioenergetic and landscape considerations for scaling expectations of nekton
520 production from intertidal marshes. Marine Ecology Progress Series, 264, 279-296.
521 Laliberte, A.S., Rango, A., 2011. Image processing and classification procedures for analysis of
522 sub-decimeter imagery acquired with an unmanned aircraft over arid rangelands.
523 GIScience & Remote Sensing 48, 4–23.
524 Laliberte, A.S., Rango, A., 2009. Texture and scale in object-based analysis of subdecimeter
525 resolution unmanned aerial vehicle (UAV) imagery. IEEE Transactions on Geoscience
526 and Remote Sensing 47, 761–770.
527 Layman, C.A., Araujo, M.S., Boucek, R., Hammerschlag-Peyer, C.M., Harrison, E., Jud, Z.R.,
528 Matich, P., Rosenblatt, A.E., Vaudo, J.J., Yeager, L.A., 2012. Applying stable isotopes to
529 examine food-web structure: an overview of analytical tools. Biological Reviews 87,
530 545–562.
531 Litvin, S.Y., Weinstein, M.P., Sheaves, M., Nagelkerken, I., 2018. What makes nearshore
532 habitats nurseries for nekton? An emerging view of the nursery role hypothesis. Estuaries
533 and Coasts 41, 1539–1550.
534 Liu, A.J., Cameron, G.N., 2001. Analysis of landscape patterns in coastal wetlands of Galveston
535 Bay, Texas (USA). Landscape Ecology 16, 581–595.
536 Manfreda, S., Dal Sasso, S.F., Pizarro, A., Tauro, F., 2019. New Insights Offered by UAS for
537 River Monitoring. Applications of Small Unmanned Aircraft Systems: Best Practices and
538 Case Studies 211.
539 Miller, M., 2014. Operations, Maintenance, and Monitoring Report for Sabine Refuge Marsh
540 Creation (CS-28). Coastal Protection and Restoration Authority of Louisiana, Coastal
541 Protection and Restoration, Lafayette, Louisiana. 25pp.

542 Minello, T.J., Zimmerman, R.J., Medina, R., 1994. The importance of edge for natant
543 macrofauna in a created salt marsh. Wetlands 14, 184–198.
544 Moore, J.C., de Ruiter, P.C., 2012. Energetic food webs: an analysis of real and model
545 ecosystems. OUP Oxford.
546 Neckles, H.A., Dionne, M., Burdick, D.M., Roman, C.T., Buchsbaum, R., Hutchins, E., 2002. A
547 monitoring protocol to assess tidal restoration of salt marshes on local and regional
548 scales. Restoration Ecology 10, 556–563.
549 Nelson, J.A., Lesser, J., James, W.R., Behringer, D.P., Furka, V., Doerr, J.C., 2019. Food web
550 response to foundation species change in a coastal ecosystem. Food Webs 21, e00125.
551 https://doi.org/10.1016/j.fooweb.2019.e00125
552 Oniga, V.-E., Breaban, A.-I., Statescu, F., 2018. Determining the optimum number of ground
553 control points for obtaining high precision results based on UAS images. Presented at the
554 Multidisciplinary Digital Publishing Institute Proceedings, p. 352.
555 Pajares, G., 2015. Overview and current status of remote sensing applications based on
556 unmanned aerial vehicles (UAVs). Photogrammetric Engineering & Remote Sensing 81,
557 281–330.
558 Palmer, M.A., Ambrose, R.F., Poff, N.L., 1997. Ecological theory and community restoration
559 ecology. Restoration ecology 5, 291–300.
560 Parnell, A.C., Phillips, D.L., Bearhop, S., Semmens, B.X., Ward, E.J., Moore, J.W., Jackson,
561 A.L., Grey, J., Kelly, D.J., Inger, R., 2013. Bayesian stable isotope mixing models.
562 Environmetrics 24. https://doi.org/10.1002/env.2221

563 Phillips, D.L., Inger, R., Bearhop, S., Jackson, A.L., Moore, J.W., Parnell, A.C., Semmens, B.X.,
564 Ward, E.J., 2014. Best practices for use of stable isotope mixing models in food-web
565 studies. Canadian Journal of Zoology 92, 823–835.
566 Pontiff DJ, White J (2017) 2016/2017 Annual Inspection Report: Sabine Refuge Marsh Creation
567 Project (CS-28-4&5). Coastal Protection and Restoration Authority
568 Prach, K., Bartha, S., Joyce, C.B., Pyšek, P., Van Diggelen, R., Wiegleb, G., 2001. The role of
569 spontaneous vegetation succession in ecosystem restoration: a perspective. Applied
570 Vegetation Science 4, 111–114.
571 Rezek, R.J., Lebreton, B., Roark, E.B., Palmer, T.A., Pollack, J.B., 2017a. How does a restored
572 oyster reef develop? An assessment based on stable isotopes and community metrics.
573 Marine biology 164, 54.
574 Rezek, R.J., Lebreton, B., Sterba-Boatwright, B., Pollack, J.B., 2017b. Ecological structure and
575 function in a restored versus natural salt marsh. PloS one 12.
576 Rozas, L.P., Minello, T.J., 1997. Estimating densities of small fishes and decapod crustaceans in
577 shallow estuarine habitats: a review of sampling design with focus on gear selection.
578 Estuaries 20, 199–213.
579 Sharp LA (2011) 2011 operations, maintenance, and monitoring report for Sabine Refuge Marsh
580 Creation. CPRA/Office of Coastal Protection and Restoration
581 Stagg, C.L., Osland, M.J., Moon, J.A., Hall, C.T., Feher, L.C., Jones, W.R., Couvillion, B.R.,
582 Hartley, S.B., Vervaeke, W.C., 2019. Quantifying hydrologic controls on local- and
583 landscape-scale indicators of coastal wetland loss. Annals of Botany 125, 365–376.
584 https://doi.org/10.1093/aob/mcz144

585 Steyer, G.D., 2010. Coastwide Reference Monitoring System (CRMS) (No. 2327–6932). US
586 Geological Survey.
587 Stock, B.C., Jackson, A.L., Ward, E.J., Parnell, A.C., Phillips, D.L., Semmens, B.X., 2018.
588 Analyzing mixing systems using a new generation of Bayesian tracer mixing models.
589 PeerJ 6, e5096.
590 Suding, K.N., 2011. Toward an era of restoration in ecology: successes, failures, and
591 opportunities ahead. Annual Review of Ecology, Evolution, and Systematics 42, 465–
592 465.
593 Suir, G.M., Evers, D.E., Steyer, G.D., Sasser, C.E., 2013. Development of a reproducible method
594 for determining quantity of water and its configuration in a marsh landscape. Journal of
595 Coastal Research 63, 110–117.
596 Suir GM, Sasser CE, Harris JM, In Review. Use of remote sensing and field data to quantify the
597 performance of restored Louisiana wetlands. Wetlands
598
599 Taddeo, S., Dronova, I., Depsky, N., 2019. Spectral vegetation indices of wetland greenness:
600 Responses to vegetation structure, composition, and spatial distribution. Remote Sensing
601 of Environment 234, 111467.
602 Vander Zanden, M.J., Olden, J.D., Gratton, C., 2006. Food-web approaches in restoration
603 ecology. Foundations of restoration ecology 165–189.
604 Webb, S., Kneib, R.T., 2004. Individual growth rates and movement of juvenile white shrimp
605 (Litopenaeus setiferus) in a tidal marsh nursery. Fishery Bulletin 102, 376–388.
606 Webb, S.R., Kneib, R., 2002. Abundance and distribution of juvenile white shrimp Litopenaeus
607 setiferus within a tidal marsh landscape. Marine Ecology Progress Series 232, 213–223.
608 Wiens, J.A., Chr, N., Van Horne, B., Ims, R.A., 1993. Ecological mechanisms and landscape
609 ecology. Oikos 369–380.

610 Wortley, L., Hero, J., Howes, M., 2013. Evaluating ecological restoration success: a review of
611 the literature. Restoration ecology 21, 537–543.
612 Zedler, J.B., Kercher, S., 2005. WETLAND RESOURCES: Status, Trends, Ecosystem Services,
613 and Restorability. Annual Review of Environment and Resources 30, 39–74.
614 https://doi.org/10.1146/annurev.energy.30.050504.144248
615

Tables

Table 1:

Site	Class	Class Area (ha)	Percentage of Landscape	Patch Density	Aggregation Index
Cycle 5	Land	67.6	73.2	718	99.9
Cycle 5	Water	24.7	26.8	880	99.7
Cycle 2	Land	119.3	86.5	529	99.8
Cycle 2	Water	18.7	13.5	3199	99.1
Cycle 3	Land	80.9	86.4	6212	99.9
Cycle 3	Water	12.7	13.6	773	99.2
Cycle 1	Land	102.9	95.5	168	99.9
Cycle 1	Water	4.9	4.5	435	98.8
Reference North	Land	44.8	91	1339	99.9
Reference North	Water	4.5	9	1327	98.8
Reference South	Land	61.0	91.8	1957	99.9
Reference South	Water	5.4	8.2	515	98.8

Figure Captions

Figure 1: Satellite image of the reference and restoration sites in Sabine, LA

Figure 2: Land and water classifications from UAS imagery overlaid on satellite imagery to show the geographic location of each site.

Figure 3: a) Cycle 1 UAS classified imagery and calculated *E*-scape map, b) Cycle 2 UAS classified imagery and calculated *E*-scape map, c) Reference South UAS classified imagery and calculated *E*-scape map. Each map is made to show the energetic landscape for white shrimp (*Litopenaeus setiferus*). Each cell in the *E*-scape maps is 400 m × 400 m and the maps are clipped to the restoration site. Areas in red indicate habitats cells that have higher energetic values and areas in blue are less energetically favorable for shrimp foraging.

Figure 4: Index of Energetic importance values for 20 random points sampled in each site. Higher values for a habitat type indicate greater energetic importance for white shrimp at that site.

Figure 5: A) Regression of land cover, B) Marsh Cover, C) Edge habitat indicating that marsh edge and the interface between land and water are the most important factors to consider for food web restoration.

Figures

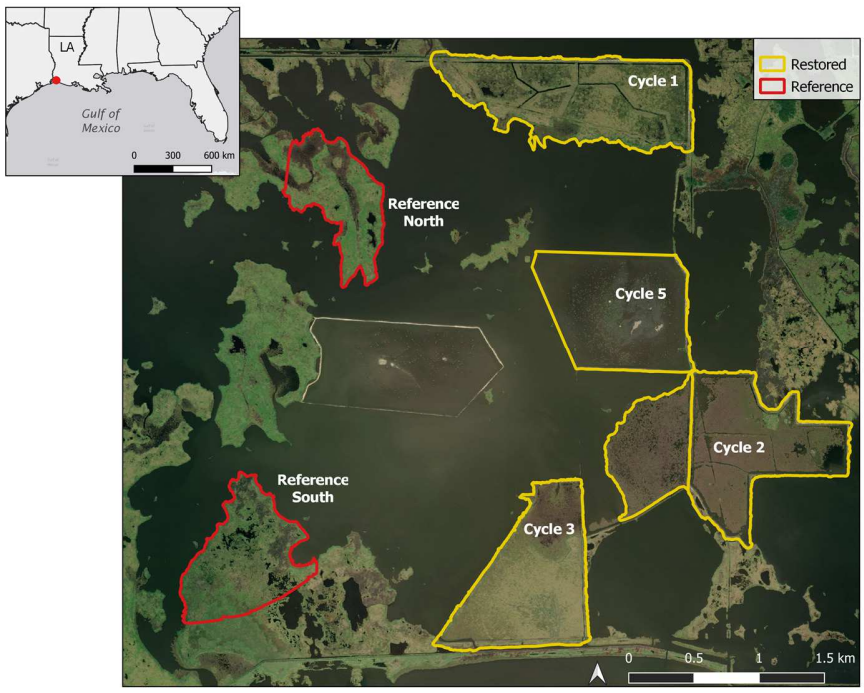

Figure 1

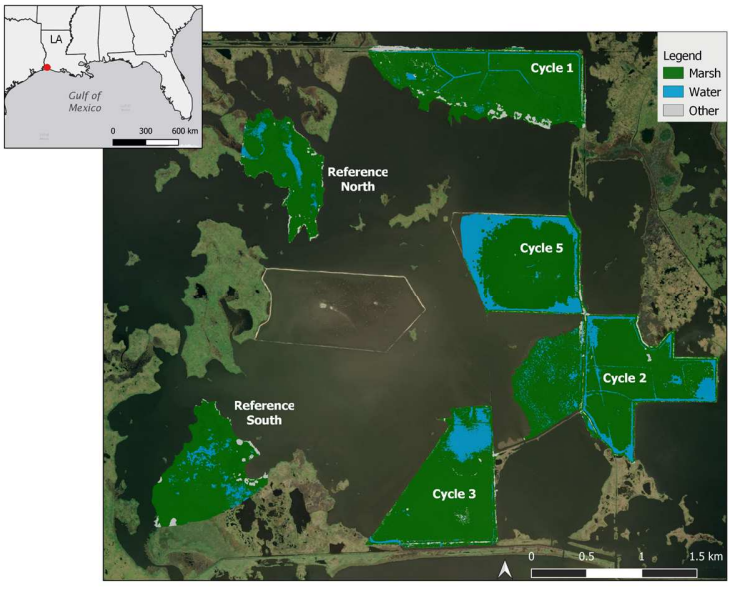

Figure 2

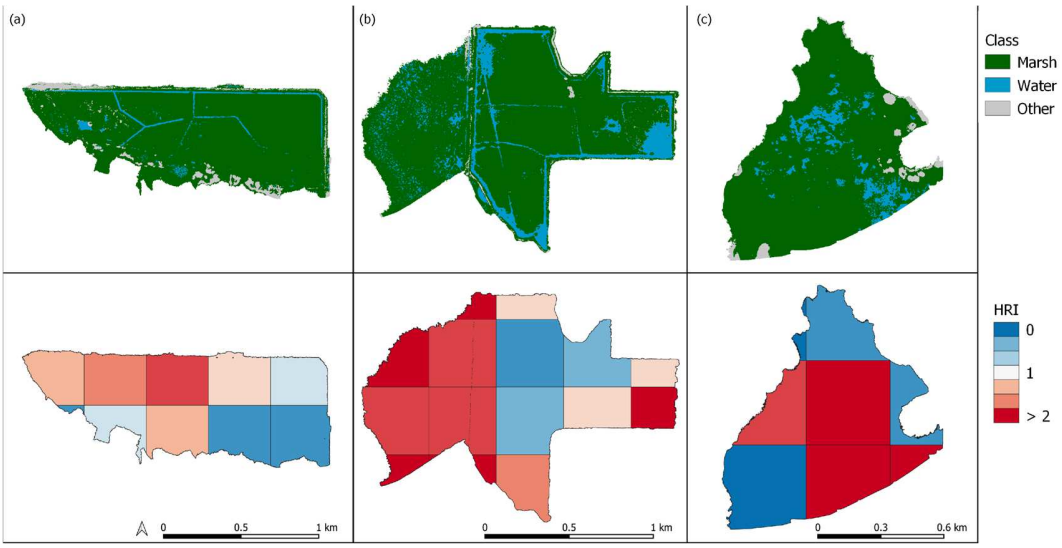

Figure 3

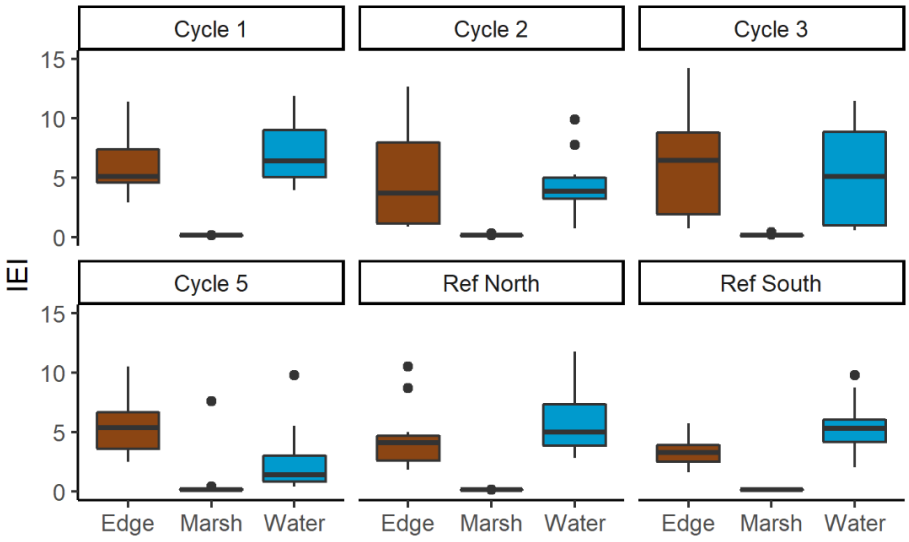

Figure 4

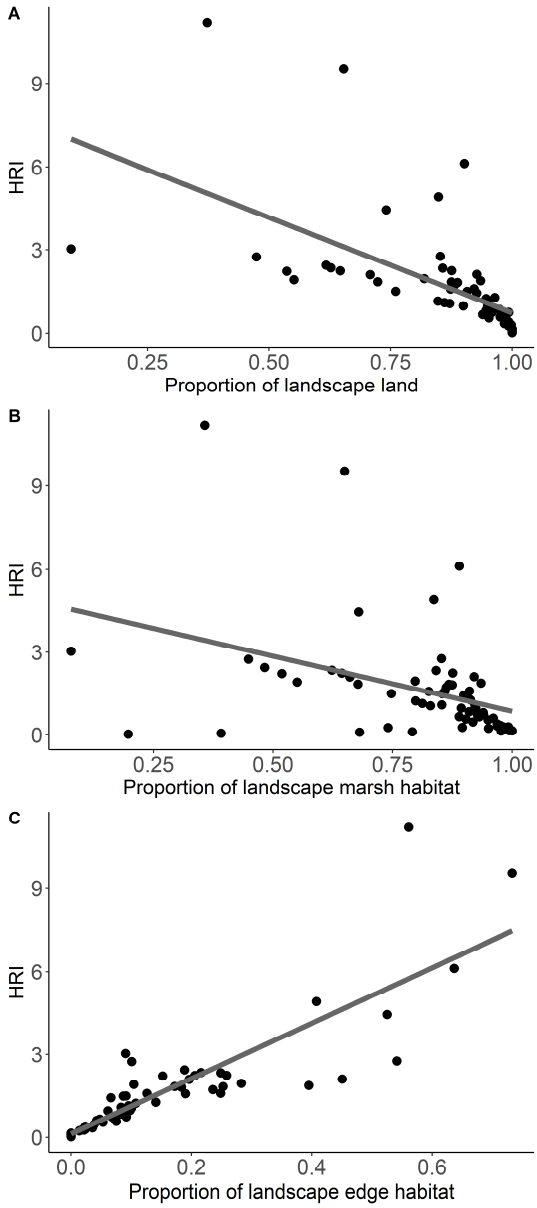
A
HRI
0
3
6
9
0.25
0.50
0.75
1.00
Proportion of landscape land
B
HRI
0
3
6
9
0.25
0.50
0.75
1.00
Proportion of landscape marsh habitat
C
HRI
0
3
6
9
0.0
0.2
0.4
0.6
Proportion of landscape edge habitat

Figure 5